



# Activated carbon/CoFe<sub>2</sub>O<sub>4</sub> composites: Facile synthesis, magnetic performance and their potential application for the removal of malachite green from water

Lunhong Ai\*, Haiyan Huang, Zhonglan Chen, Xing Wei, J. Jiang

Laboratory of Applied Chemistry and Pollution Control Technology, College of Chemistry and Chemical Engineering, China West Normal University, Shida Road 1#, Nanchong 637002, China

## ARTICLE INFO

### Article history:

Received 5 February 2009

Received in revised form 15 August 2009

Accepted 28 August 2009

### Keywords:

Activated carbon

CoFe<sub>2</sub>O<sub>4</sub>

Malachite green

Magnetic performance

Dye removal

## ABSTRACT

Activated carbon/CoFe<sub>2</sub>O<sub>4</sub> composite (AC/CFO) was synthesized by a simple one-step refluxing route and was used as adsorbent for the removal of malachite green (MG) dye from water. The structure, morphology and magnetic properties of as-prepared composite were characterized by X-ray diffractometer (XRD), scanning electron microscope (SEM), transmission electron microscope (TEM) and vibrating sample magnetometer (VSM). The results indicated that CoFe<sub>2</sub>O<sub>4</sub> particles deposited on the surface of activated carbon in the composite were uniform with the particle size in the range of 14–20 nm. The composite adsorbents exhibited a clearly hysteretic behavior under applied magnetic field, which allowed their magnetic separation from water. Batch experiments were carried out to investigate adsorption isotherms and kinetics of MG onto the composite. The experimental data fitted well with the Langmuir model with a monolayer adsorption capacity of 89.29 mg g<sup>-1</sup>. The adsorption kinetics was found to follow pseudo-second-order kinetic model. It was indicated that the as-prepared composite could be used as a promising and effective adsorbent for the removal of MG from water.

© 2009 Elsevier B.V. All rights reserved.

## 1. Introduction

In recent years, increasing concern for public health and environmental quality has led to a growth of special interest in developing and implementing various methods of removing potentially toxic organic and inorganic pollutants from water [1]. Dyes from a wide variety of sources, such as textiles, printing, dyeing, dyestuff manufacturing and food plants, which represent a significant threat to the ecosystem, are major sources of environmental pollution and recognized as difficult-to-treat pollutants [2].

Malachite green (MG), tri-phenyl methane dye, has been widely used for the dyeing of leather, wool and silk as well as in distilleries [3]. In addition, MG also is used as a fungicide and antiseptic in aquaculture industry to control fish parasites and disease [4]. However, MG is very dangerous and highly cytotoxic to mammalian cells, and also acts as a liver tumor-enhancing agent. The dye which is released aquatic environment without any treatments inhibits development of aquatic animals and plants by blocking out sunlight penetration [5,6]. Therefore, there is considerable need to treat these effluents prior to their discharge into receiving waters to prevent environmental pollution in the aquatic ecosystems.

Several methods have been developed to remove color from dyehouse effluents, varying in effectiveness, economic cost, and environmental impact (of the treatment process itself). Among all of the treatments proposed, the adsorption of dye molecules onto a substrate (adsorbent) can be a very effective, low-cost method of color removal [7–9]. Activated carbons offer an attractive and inexpensive option for the efficient removal of various organic contaminants from water due to its high surface area and porous structure [10–12]. However, filtration, the traditional method for separating activated carbon, may cause the blockage of filters or the loss of carbon. Therefore, activated carbon has been traditionally discarded with the process sludge after use in water and wastewater treatment, resulting in the secondary pollution [13,14]. Thus, the difficulties encounter in separating spent activated carbon and regeneration limit its applications in many fields.

Magnetic separation is considered as a quick and effective technique for separating magnetic particles. It has been used for many applications in biochemistry, analytical chemistry and mining ores. Recently, considerable attention has been focused on the application of magnetic separation technology to solve environmental problems. Qu et al. have synthesized multi-walled carbon nanotubes filled with Fe<sub>2</sub>O<sub>3</sub> particles as the magnetic adsorbent for the removal of dyes [15]. Gong et al. have employed magnetic multi-wall carbon nanotube nanocomposite as adsorbent for the removal of cationic dyes [16]. Yang et al. have developed magnetic Fe<sub>3</sub>O<sub>4</sub>-activated carbon nanocomposite particles for the removal of

\* Corresponding author. Tel.: +86 817 2568081; fax: +86 817 2224217.  
E-mail address: [ah.aihong@163.com](mailto:ah.aihong@163.com) (L. Ai).

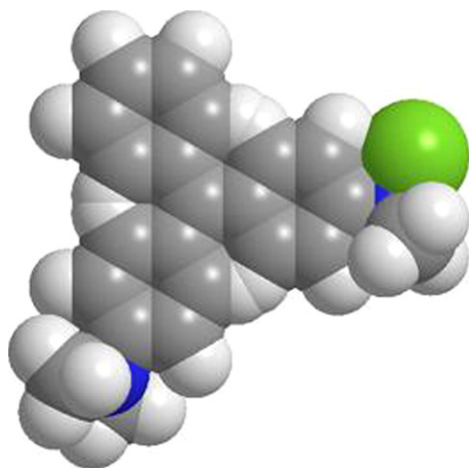


**Fig. 1.** Three-dimensional molecular structure of malachite green (dark gray, carbon atoms; light gray, hydrogen atoms; green, chloride atoms; and blue, nitrogen atoms). (For interpretation of the references to color in this figure legend, the reader is referred to the web version of the article.)

methylene blue from aqueous solution [17]. Rocher et al. have prepared magnetic alginate beads containing magnetic nanoparticles and activated carbon for the removal of organic dyes [18].

Ferrites of the type  $MFe_2O_4$  ( $M$  is a divalent metal cation) are magnetic materials with the cubic spinel structure, which have been extensively used in various technological applications in the past decades [19,20]. Recently, the exploitation of  $MnFe_2O_4$  and  $CuFe_2O_4$  ferrite in treatment for water has been mostly studied by Qu's group, which exhibited the excellent adsorptive properties with the highly effective recovery of the magnetic separation technique [21–24]. Among ferrites,  $CoFe_2O_4$  is an interesting magnetic material due to its moderate saturation magnetization, excellent chemical stability and mechanical hardness [25]. Therefore, combining the advantages of carbon materials and magnetic  $CoFe_2O_4$  particles to fabricate a promising novel adsorbent opens new possibilities for the achievement of desirable absorptivity and effective magnetic separability. To the best of our knowledge, little work has been done on the preparation of activated carbon/ $CoFe_2O_4$  composite and their dye removal from water. In the present study herein, a simple one-pot refluxing method was employed to develop a new kind of magnetic adsorbent, activated carbon/ $CoFe_2O_4$  composite (AC/CFO). We first address the issue of the malachite green (MG) adsorption onto magnetic AC/CFO composite from water. The evaluation of adsorption equilibrium, isotherms and kinetics of MG onto the composite was investigated as well.

## 2. Experimental

### 2.1. Materials

All the reagents were of analytical grade and used as received without further purification. Cobalt nitrate [ $Co(NO_3)_2 \cdot 6H_2O$ ], ferric nitrate [ $Fe(NO_3)_3 \cdot 9H_2O$ ], sodium hydroxide (NaOH), activated carbon (AC) and malachite green (Fig. 1) (formula:  $C_{23}H_{26}N_2Cl$ , molecular weight: 364.92;  $\lambda_{max}$ : 620 nm) were purchased from Chengdu Kelong Chemical Reagent Co. (China).

### 2.2. Preparation of activated carbon/ $CoFe_2O_4$ composite (AC/CFO)

Activated carbon/ $CoFe_2O_4$  composite was synthesized by a facile refluxing route in alkaline solution. In a typical procedure, a certain amount of activated carbon was added into a 150 mL alkaline solution containing 3.4 g NaOH, and stirred at room temperature for 30 min to get the activated carbon suspension. The

suspension was then maintained at 100 °C to keep boiling state. A 50 mL metal nitrate aqueous solution was prepared by dissolving  $Fe(NO_3)_3 \cdot 9H_2O$  (5.4944 g) and  $Co(NO_3)_2 \cdot 6H_2O$  (1.9790 g) in distilled water. The solution was poured as quickly as possible into the above boiling suspension. The mixture solution was then refluxed at 100 °C for 2 h. By a simple magnetic procedure, the resulting product was separated from water and dried at 80 °C for 12 h.

### 2.3. Characterization

The BET surface area of samples was determined by nitrogen adsorption–desorption isotherm measured at 77 K on a Micromeritics Gemini 2370 surface area analyzer. The phase identification of samples was performed on a Philips X'pert Pro MPD diffractometer with  $Cu K\alpha$  radiation ( $\lambda = 0.15418$  nm). Scanning electron microscopy (SEM) investigations were carried out on a Hitachi S4800 field emission scanning electron microscope. TEM images were obtained on a JEM-100CXII transmission electron microscope at an accelerating voltage of 200 kV. Magnetic measurements were carried out at room temperature using a vibrating sample magnetometer (VSM, Lakeshore 7404) with a maximum magnetic field of 15 kOe.

### 2.4. Adsorption experiments

Adsorption experiments were carried out with a thermostated shaker at 200 rpm. Experiments were performed using a batch equilibrium technique by placing 0.05 g of AC/CFO adsorbent in a glass bottle containing 25 mL of a dye solution at various concentrations. The experiments were carried out at different pH and contact time. The solution pH was adjusted with NaOH or HCl solutions using a Jenway pH meter. The batch adsorption experiments were conducted in duplicate.

The equilibrium concentrations of dyes were determined at 620 nm for MG using a UV–vis spectrophotometer (Shimadzu, UV-2550). The concentrations of the solutions were determined by using linear regression equation ( $y = -0.0117 + 0.1249x$ ,  $R^2 = 0.999$ ) obtained by plotting a calibration curve for dye over a range of concentrations. The amounts of MG adsorbed were determined by the difference between the initial and remaining concentrations of dye solution using the equation:

$$q = \frac{(C_0 - C_e)V}{m} \quad (1)$$

where  $C_0$  and  $C_e$  are the initial and equilibrium concentrations of dye ( $mg L^{-1}$ ),  $m$  is the mass of AC/CFO (g), and  $V$  is the volume of solution (L).

### 2.5. Desorption experiments

In order to assess the practical utility of AC/CFO adsorbents, desorption experiments were conducted. For the desorption study, 0.05 g AC/CFO adsorbents were added to 25 mL of dye solutions ( $100 mg L^{-1}$ ) with contact time of 20 min. The dye-adsorbed AC/CFO adsorbents were treated by the alcohol solution. The adsorption–desorption cycle was repeated three times by using the same AC/CFO and initial concentration used in this experiment.

## 3. Results and discussion

### 3.1. Characterization of magnetic AC/CFO composite adsorbent

The physical properties (Table 1) suggest that the BET surface area and total pore volume are affected by the presence of  $CoFe_2O_4$  in the composites. With an introduction of  $CoFe_2O_4$  supported on the activated carbon, a decrease of the surface area and total pores

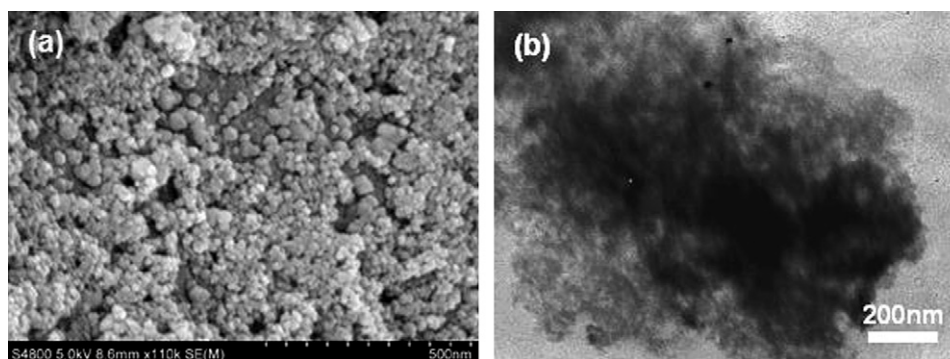


Fig. 2. SEM micrograph (a) and TEM image (b) of AC/CFO.

Table 1

Physical properties of activated carbon and AC/CFO.

Samples	BET-surface area ( $\text{m}^2 \text{g}^{-1}$ )	Total pore volume ( $\text{cm}^3 \text{g}^{-1}$ )	Saturation magnetization ( $\text{emu g}^{-1}$ )
Activated carbon	909	0.47	0
AC/CFO	463	0.18	7.6

volume are observed, since the  $\text{CoFe}_2\text{O}_4$  have a relatively small surface area and are covering the activated carbon surface [26]. The similar results have been reported in literatures for the magnetic oxide-supported activated carbon [14,17,26]. It should be mentioned that the composite retains a large surface area ( $463 \text{ m}^2 \text{ g}^{-1}$ ) and a high total porous volume ( $0.18 \text{ cm}^3 \text{ g}^{-1}$ ), indicating that the pores of the activated carbon are not blocked by the presence of magnetic  $\text{CoFe}_2\text{O}_4$ .

The morphology of the as-prepared AC/CFO was investigated by SEM and TEM observations. As shown in Fig. 2(a), it can be seen that  $\text{CoFe}_2\text{O}_4$  particles deposited on the surface of activated carbon in the composite are uniform with the particle size in the range of 14–20 nm. Fig. 2(b) shows a typical TEM image of the composite. The light colored region is activated carbon whereas black region indicates the presence of magnetic  $\text{CoFe}_2\text{O}_4$  particle in the composite, due to the different electron penetrability.

Fig. 3 shows XRD patterns of the  $\text{CoFe}_2\text{O}_4$  particles and AC/CFO. The diffraction peaks in Fig. 3(a) can be perfectly indexed to the cubic spinel structure (JCPDS card no. 22-1086), and no characteristic peaks of impurities are detected in the XRD pattern, implying that the formation of the single phase spinel. As shown in Fig. 3(b), besides a weak peak appearing at  $2\theta = 26.5^\circ$  corresponding to acti-

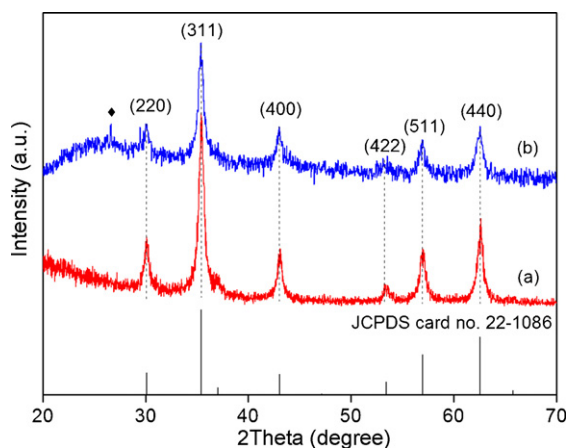


Fig. 3. XRD patterns of  $\text{CoFe}_2\text{O}_4$  (a) and AC/CFO (b); and the reference standard data for  $\text{CoFe}_2\text{O}_4$  of the JCPDS file No. 22-1086.

vated carbon, the XRD pattern of AC/CFO is almost identical to that of the  $\text{CoFe}_2\text{O}_4$  particles. Furthermore, the observed diffraction peaks are broad and less sharp, indicating as-prepared  $\text{CoFe}_2\text{O}_4$  particles with small dimensions. The average crystallite size of  $\text{CoFe}_2\text{O}_4$  particles can be estimated according to the diffraction reflections by using the Debye–Scherrer formula  $D = 0.9\lambda / \beta \cos \theta$ , where  $D$  is the average crystallite size,  $\lambda$  is the wavelength of  $\text{Cu K}\alpha$ ,  $\beta$  is the full width at half maximum (FWHM) of the diffraction peaks, and  $\theta$  is the Bragg's angle. The average crystallite sizes are estimated to be 21 and 15 nm, respectively, for bare  $\text{CoFe}_2\text{O}_4$  particles and  $\text{CoFe}_2\text{O}_4$  particles in AC/CFO.

The magnetization measurements for the as-prepared AC/CFO are carried out using a vibrating sample magnetometer (VSM) at room temperature with an applied magnetic field of 15 kOe, which reveals that AC/CFO exhibits a clearly hysteretic behavior. The magnetic hysteresis loops of the as-prepared AC/CFO, shown in Fig. 4, indicate that the values of saturation magnetization and remnant magnetization is  $7.6 \text{ emu g}^{-1}$  and  $1.4 \text{ emu g}^{-1}$ , respectively, which are lower than those of the bare  $\text{CoFe}_2\text{O}_4$  particles due to the existence of AC. The magnetic separability of the AC/CFO is also tested by placing a magnet near the glass bottle. The black product is attracted toward the magnet in a short period (inset in Fig. 4), demonstrating high magnetic sensitivity of our product. These results show that AC/CFO can be potentially used as a magnetic adsorbent to remove contaminants in water.

### 3.2. Adsorption and removal of MG dye

#### 3.2.1. Effect of pH

The pH of the dye solution plays an important role in the whole adsorption process. To determine the optimum pH conditions for

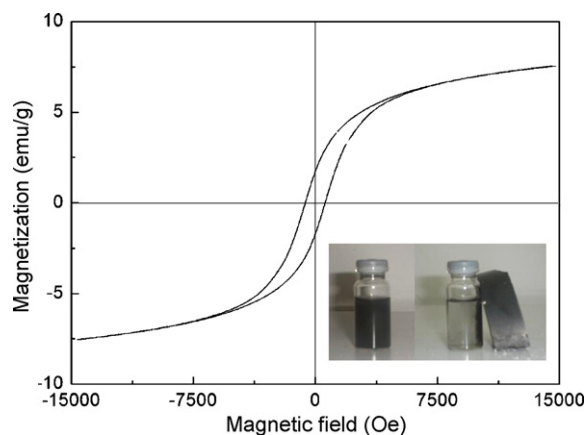


Fig. 4. Magnetic hysteresis loops of AC/CFO at 300 K; the inset of figure shows the well-dispersed solution by magnetic separation under an external magnetic field.

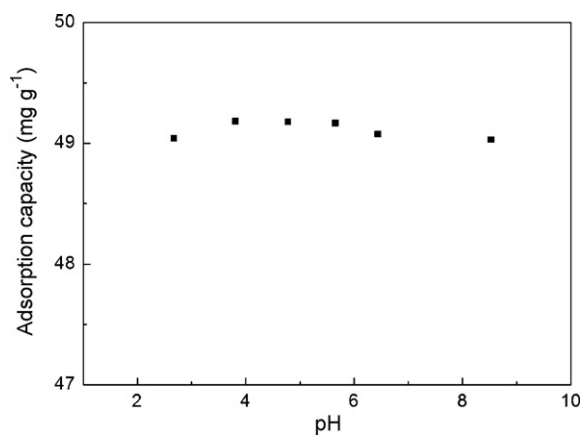


Fig. 5. Effect of pH on adsorption of MG onto AC/CFO ( $C_0$ : 100 mg L<sup>-1</sup>; contact time: 20 min).

adsorption of MG onto AC/CFO, the effect of solution pH on the adsorption of dye is investigated in the range of 2–9 with a fixed initial concentration (100 mg L<sup>-1</sup>) and contact time (20 min), as shown in Fig. 5. The adsorption capacities of MG by AC/CFO present a relatively low at pH less than 3, and increase up to pH 5. Solution pH may affect both aqueous chemistry and surface binding-sites of the adsorbent. The decrease of adsorption at pH less than 3 can be explained by the fact that at this acidic pH, H<sup>+</sup> may compete with dye ions for the adsorption sites of adsorbent, thereby inhibiting the adsorption of dye [27].

### 3.2.2. Adsorption isotherms

The equilibrium adsorption isotherm is fundamental in describing the interactive behavior between solutes and adsorbent, and is important for the design of adsorption system. Fig. 6 shows the adsorption isotherms of MG onto AC/CFO. The adsorption capacities of MG increase with increasing of the dye concentration. It is clearly seen from Fig. 6 that the shape of the isotherm reveals L-behavior according to the Giles classification [28], confirming a high affinity between AC/CFO and the dye molecule. The initial sharp rise indicates that a large amount of dye is adsorbed at a lower concentration as more active sites of AC/CFO are available. As the concentration increases, it becomes difficult for a dye molecule to find vacant sites, and so monolayer formation occurs.

The equilibrium adsorption data are analyzed using the well-known Langmuir and Freundlich models. A basic assumption of the Langmuir theory is that sorption takes place at specific homogeneous sites within the adsorbent. Compared to the Langmuir

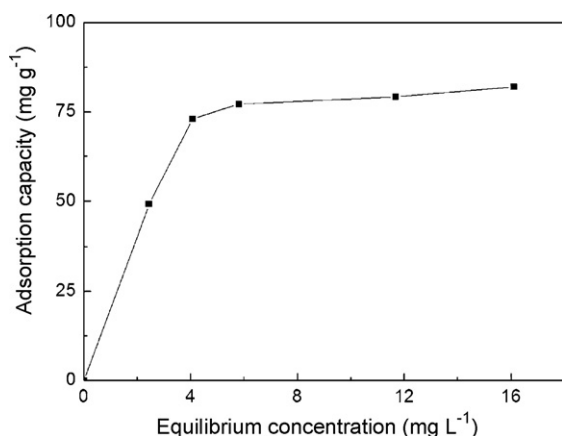


Fig. 6. Adsorption isotherms of MG onto AC/CFO.

Table 2

Langmuir and Freundlich model parameters for adsorption MG onto AC/CFO.

Langmuir			Freundlich			
$b$ (L mg <sup>-1</sup> )	$q_m$ (mg g <sup>-1</sup> )	$R^2$	$R_L$	$K_f$ (mg g <sup>-1</sup> )	$n$	$R^2$
0.752	89.29	0.988	0.007–0.013	46.635	4.434	0.458

isotherm, the Freundlich model is generally found to be better suited for characterizing multi-layer adsorption process. The linear forms of the Langmuir and Freundlich models are represented by the following equations, respectively [29,30]:

$$\frac{C_e}{q_e} = \frac{1}{bq_m} + \frac{C_e}{q_m} \quad (2)$$

$$q_e = K_f C_e^{1/n} \quad (3)$$

where  $q_m$  (mg g<sup>-1</sup>) and  $b$  (L mg<sup>-1</sup>) are Langmuir isotherm coefficients. The value of  $q_m$  represents the monolayer adsorption capacity.  $K_f$  (mg g<sup>-1</sup>) and  $n$  are Freundlich constants.

The Langmuir equation parameters for the MG adsorption are summarized in Table 2. The linearization of the equations and the values of correlation coefficient ( $R^2$ ) are  $y = 0.0149 + 0.0112x$ , 0.988, respectively. The  $q_m$  values for the adsorption of MG is 89.29 mg g<sup>-1</sup>, in accordance with the experimental value obtained, 81.94 mg g<sup>-1</sup>. Table 3 compares the monolayer adsorption capacities of AC/CFO obtained in this study with different adsorbents previously used for the removal of MG dye. It can be seen from Table 3 that the adsorption capacities of AC/CFO for MG dye are much higher than that of many other previously reported adsorbents, indicating that the as-prepared AC/CFO has great potential for application in MG dye removal from water.

The Freundlich equation parameters for the MG adsorption estimated using linear regression are shown in Table 2. The value of correlation coefficient ( $R^2$ ) of Freundlich model is lower than Langmuir value, indicating that the adsorption process should be better represented by Langmuir isotherm model than Freundlich isotherm model.

For the Langmuir-type adsorption process, the influence of the isotherm shape on whether adsorption is favorable or unfavorable can be classified by the separation factor  $R_L$ , which is considered as a more reliable indicator of the adsorption capacity [39]. This constant is evaluated as:

$$R_L = \frac{1}{1 + bC_0} \quad (4)$$

where  $b$  (L mg<sup>-1</sup>) is the Langmuir constant and  $C_0$  (mg L<sup>-1</sup>) is the initial concentration. Favorable adsorption is reported when the  $R_L$ -values are between 0 and 1 [40]. In the present work, the  $R_L$ -values of the MG adsorption by AC/CFO are in the ranges of 0.007–0.013 (Table 2) shows that the adsorption process is favorable.

Table 3

Comparison of the monolayer adsorption capacities ( $q_m$ ) of MG onto various adsorbents.

Adsorbents	$q_m$ (mg g <sup>-1</sup> )	References
AC/CFO	89.29	This study
Lemon peel	51.73	[31]
Zeolite	46.35	[32]
Bentonite	7.72	[33]
Cyclodextrin-based adsorbent	91.90	[34]
Jute fiber carbon	136.59	[35]
Arundo donax root carbon (ADRC)	8.49	[4]
<i>Caulerpa racemosa</i> var. <i>cylindracea</i> (CRC)	25.67	[5]
Activated slag	74.2	[36]
Hen feathers	26.1	[37]
Bagasse fly ash	170.3	[38]

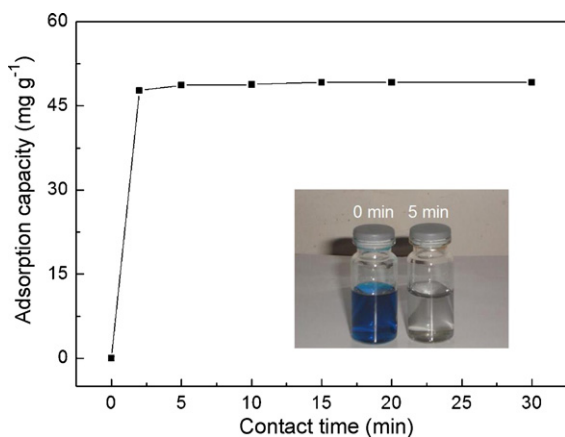


Fig. 7. Effect of contact time on adsorption of MG onto AC/CFO ( $C_0$ :  $100 \text{ mg L}^{-1}$ ; pH 5); and the inset of figure shows the change in color of MG in the presence of AC/CFO in aqueous solution.

### 3.2.3. Adsorption kinetics

The effect of contact time on adsorption of MG onto AC/CFO is investigated for initial dye concentration of  $100 \text{ mg L}^{-1}$ , as shown in Fig. 7. The adsorption capacities of AC/CFO increase rapidly in the initial stages of contact time and reach equilibrium at 20 min. The results indicate that at the beginning the adsorption rate is fast as the dye is adsorbed by the exterior surface of AC/CFO. When the adsorptions of the exterior surface reach saturation, the dye exerts onto the pores of the adsorbent and is adsorbed by the interior surface of the adsorbent. The inset in Fig. 7 shows photographs of the MG adsorption by AC/CFO with contact time 0 min and 5 min, which indicates the rapid decoloration of MG by obtained AC/CFO adsorbent.

To investigate the adsorption mechanism of MG on the surface of AC/CFO, two kinetic models, pseudo-first-order and pseudo-second-order kinetic model, were tested to find the best fitted model for the experimental data.

The pseudo-first-order Lagergren equation is given by [41]:

$$\log(q_e - q_t) = \log q_e - \frac{k_1 t}{2.303} \quad (5)$$

where  $k_1$  is the pseudo-first-order rate constant ( $\text{min}^{-1}$ ),  $q_e$  and  $q_t$  are the amounts of dye adsorbed ( $\text{mg g}^{-1}$ ) at equilibrium and at time  $t$  (min).

The pseudo-second-order model can be expressed as [42]:

$$\frac{t}{q_t} = \frac{1}{k_2 q_e^2} + \frac{t}{q_e} \quad (6)$$

where  $k_2$  ( $\text{g mg}^{-1} \text{ min}^{-1}$ ) is the rate constant of the pseudo-second-order adsorption. The initial adsorption rate in the pseudo-second-order kinetic model is  $h = tq_e^2$ .

Kinetic constants obtained by linear regression (Figs. 8 and 9) for the two models are listed in Table 4. The correlation coefficient for the pseudo-first-order model is relatively high ( $R^2 = 0.951$ ), however, the calculated  $q_e$  value ( $q_{e,\text{cal}}$ ) value obtained from this equation does not give reasonable value (Table 4), which is much lower compared with experimental data ( $q_{e,\text{exp}}$ ). This result suggests that the adsorption process does not follow the pseudo-first-order kinetic model, which is similar to the result reported for

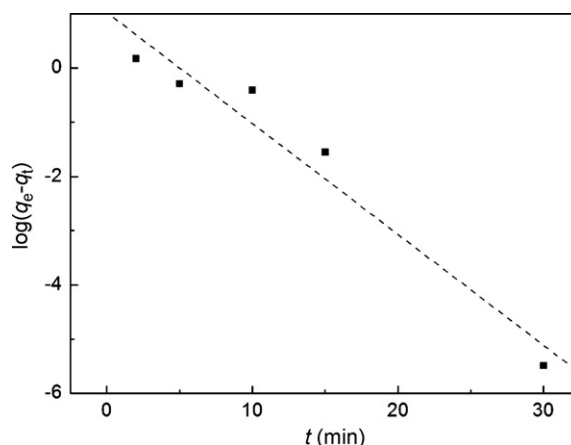


Fig. 8. Pseudo-first-order kinetic plots for adsorption of MG onto AC/CFO ( $C_0$ :  $100 \text{ mg L}^{-1}$ , pH 5).

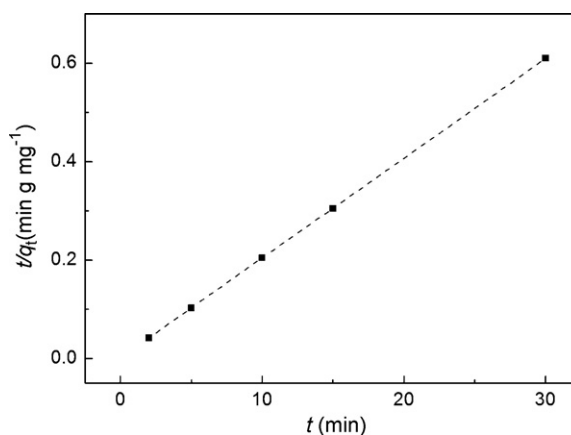


Fig. 9. Pseudo-second-order kinetic plots for adsorption of MG onto AC/CFO ( $C_0$ :  $100 \text{ mg L}^{-1}$ , pH 5).

adsorption of MG onto bentonite [43]. In many cases the pseudo-first-order equation of Lagergren does not fit well to the whole range of contact time and is generally applicable over the initial stage of the adsorption processes [44,45]. For the pseudo-second-order kinetic model, the  $R^2$  value is 1 and the  $q_{e,\text{cal}}$  value agrees very well with the  $q_{e,\text{exp}}$  value, which indicates that the adsorption of MG onto AC/CFO follows a pseudo-second-order kinetic model.

### 3.3. Desorption study

To evaluate the possibility of regeneration of AC/CFO adsorbent, we have performed desorption experiments. The cycles of adsorption–desorption experiments were carried out up to three times, as shown in Fig. 10. It can be seen that the adsorption capacities decrease for each new cycle after desorption with three cycles. Meanwhile, AC/CFO adsorbent has high magnetic sensitivity under an external magnetic field (inset in Fig. 4). These results show that AC/CFO can be potentially used as a magnetic adsorbent to remove dye contaminants from water for avoiding the secondary pollution.

Table 4  
Kinetic parameters for adsorption MG onto AC/CFO.

$q_{e,\text{exp}}$ ( $\text{mg g}^{-1}$ )	Pseudo-first-order			Pseudo-second-order			
	$k_1$ ( $\text{min}^{-1}$ )	$q_{e,\text{cal}}$ ( $\text{mg g}^{-1}$ )	$R^2$	$k_2$ ( $\text{g mg}^{-1} \text{ min}^{-1}$ )	$q_{e,\text{cal}}$ ( $\text{mg g}^{-1}$ )	$h$ ( $\text{mg g}^{-1} \text{ min}^{-1}$ )	$R^2$
49.21	0.471	10.55	0.951	0.283	49.33	688.7	1

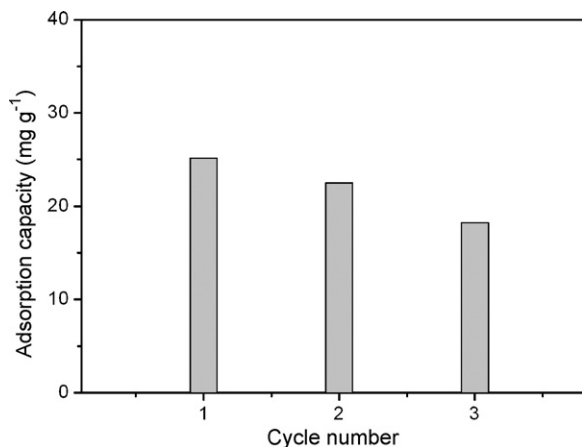


Fig. 10. Adsorption-desorption cycles of AC/CFO.

#### 4. Conclusions

In this study, activated carbon/CoFe<sub>2</sub>O<sub>4</sub> composite (AC/CFO) was successfully synthesized by a facile one-step refluxing route. The XRD, SEM, TEM, BET surface area and magnetic measurements were used to characterize the as-prepared composite. The adsorption isotherms and kinetics of MG onto AC/CFO was investigated. The equilibrium of adsorption of MG onto AC/CFO was suitably described by the Langmuir models with a monolayer adsorption capacity of 89.29 mg g<sup>-1</sup>. The process of adsorption was relatively rapid and was best described by the pseudo-second-order kinetic model. AC/CFO adsorbents could be regenerated and used repeatedly. The magnetic properties of AC/CFO adsorbents allowed their separation from water by applying a magnetic field, indicating that AC/CFO could be used as a promising and effective adsorbent for the removal of MG dye from water.

#### Acknowledgements

This work was supported by Scientific Research Start-up Foundation of China West Normal University (07B005) and Student Science & Technology Innovation Project of China West Normal University.

#### References

- [1] A.-N. Chowdhury, S.R. Jesmeen, M.M. Hossain, Removal of dyes from water by conducting polymeric adsorbent, *Polym. Adv. Technol.* 15 (2004) 633–638.
- [2] A. Bhatnagar, A.K. Jain, A comparative adsorption study with different industrial wastes as adsorbents for removal of cationic dyes from water, *J. Colloid Interface Sci.* 281 (2005) 49–55.
- [3] W. Cheng, S.-G. Wang, L. Lu, W.-X. Gong, X.-W. Liu, B.-Y. Gao, H.-Y. Zhang, Removal of malachite green (MG) from aqueous solutions by native and heat-treated anaerobic granular sludge, *Biochem. Eng. J.* 39 (2008) 538–546.
- [4] J. Zhang, Y. Li, C. Zhang, Y. Jing, Adsorption of malachite green from aqueous solution onto carbon prepared from *Arundo donax* root, *J. Hazard. Mater.* 150 (2008) 774–782.
- [5] Z. Bekci, Y. Seki, L. Cavas, Removal of malachite green by using an invasive marine alga *Caulerpa racemosa* var. *cylindracea*, *J. Hazard. Mater.* 161 (2009) 1454–1460.
- [6] S.P. Raghuvanshi, R. Singh, C.P. Kaushik, Kinetics study of methylene blue dye bioadsorption on baggase, *Appl. Ecol. Environ. Res.* 2 (2004) 35–43.
- [7] G. San Miguel, S.D. Lambert, N. Graham, A practical review of the performance of organic and inorganic adsorbents for the treatment of contaminated waters, *J. Chem. Technol. Biotechnol.* 81 (2006) 1685–1696.
- [8] G. Crini, Non-conventional low-cost adsorbents for dye removal: a review, *Bioresour. Technol.* 97 (2006) 1061–1085.
- [9] A. Bhatnagar, A.K. Minocha, Conventional non-conventional adsorbents for removal of pollutants from water—a review, *Indian J. Chem. Technol.* 13 (2006), pp. 203–127.
- [10] I. Martyn-Gullon, R. Font, Dynamic pesticide removal with activated carbon fibers, *Water Res.* 35 (2001) 516–520.

- [11] P. Pendleton, S.H. Wu, Kinetics of dodecanoic acid adsorption from caustic solution by activated carbon, *J. Colloid Interface Sci.* 226 (2003) 245–250.
- [12] I.A. Garner, I.A. Watson-Craik, R. Kirkwood, Dual solute adsorption of 2,4,6-trichlorophenol and *N*-[2-(2,4,6-trichlorophenoxy)propyl]amine onto activated carbon, *J. Chem. Technol. Biotechnol.* 76 (2001) 932–940.
- [13] D. Clifford, P. Chu, A. Lau, Thermal regeneration of powdered activated carbon (PAC) and PAC-biological sludge mixtures, *Water Res.* 17 (1983) 1125–1138.
- [14] G. Zhang, J. Qu, H. Liu, A.T. Cooper, R. Wu, CuFe<sub>2</sub>O<sub>4</sub>/activated carbon composite: a novel magnetic adsorbent for the removal of acid orange II and catalytic regeneration, *Chemosphere* 68 (2007) 1058–1066.
- [15] S. Qu, F. Huang, S. Yu, G. Chen, J. Kong, Magnetic removal of dyes from aqueous solution using multi-walled carbon nanotubes filled with Fe<sub>2</sub>O<sub>3</sub> particles, *J. Hazard. Mater.* 160 (2008) 643–647.
- [16] J.-L. Gong, B. Wang, G.-M. Zeng, C.-P. Yang, C.-G. Niu, Q.-Y. Niu, W.-J. Zhou, Y. Liang, Removal of cationic dyes from aqueous solution using magnetic multi-wall carbon nanotube nanocomposite as adsorbent, *J. Hazard. Mater.* 164 (2009) 1517–1522.
- [17] N. Yang, S. Zhu, D. Zhang, S. Xu, Synthesis and properties of magnetic Fe<sub>3</sub>O<sub>4</sub>-activated carbon nanocomposite particles for dye removal, *Mater. Lett.* 62 (2008) 645–647.
- [18] V. Rocher, J.-M. Siaugue, V. Cabuil, A. Bee, Removal of organic dyes by magnetic alginate beads, *Water Res.* 42 (2008) 1290–1298.
- [19] B. Baruwati, M.N. Nadagouda, R.S. Varma, Bulk synthesis of monodisperse ferrite nanoparticles at water-organic interfaces under conventional and microwave hydrothermal treatment and their surface functionalization, *J. Phys. Chem. C* 112 (2008) 18399–18404.
- [20] Q. Song, Z.J. Zhang, Shape control and associated magnetic properties of spinel cobalt ferrite nanocrystals, *J. Am. Chem. Soc.* 126 (2004) 6164–6168.
- [21] G. Zhang, H. Liu, R. Liu, J. Qu, Removal of phosphate from water by a Fe-Mn binary oxide adsorbent, *J. Colloid Interface Sci.* 335 (2009) 168–174.
- [22] G. Zhang, J. Qu, H. Liu, R. Liu, R. Wu, Preparation and evaluation of a novel Fe-Mn binary oxide adsorbent for effective arsenite removal, *Water Res.* 41 (2007) 1921–1928.
- [23] R. Wu, J. Qu, Removal of water-soluble azo dye by the magnetic material MnFe<sub>2</sub>O<sub>4</sub>, *J. Chem. Technol. Biotechnol.* 80 (2005) 20–27.
- [24] R. Wu, J. Qu, H. He, Y. Yu, Removal of azo-dye Acid Red B (ARB) by adsorption and catalytic combustion using magnetic CuFe<sub>2</sub>O<sub>4</sub> powder, *Appl. Catal. B* 48 (2004) 49–56.
- [25] X.-M. Liu, S.-Y. Fu, L.-P. Zhu, High-yield synthesis and characterization of monodisperse sub-microsized CoFe<sub>2</sub>O<sub>4</sub> octahedra, *J. Solid State Chem.* 180 (2007) 461–466.
- [26] C.S. Castro, M.C. Guerreiro, M. Goncalves, L.C.A. Oliveira, A.S. Anastacio, Activated carbon/iron oxide composites for the removal of atrazine from aqueous medium, *J. Hazard. Mater.* 164 (2009) 609–614.
- [27] B.H. Hameed, M.I. El-Khaiary, Malachite green adsorption by rattan sawdust: isotherm, kinetic and mechanism modeling, *J. Hazard. Mater.* 159 (2008) 574–579.
- [28] C.H. Giles, T.H. MacEwan, S.M. Nakhwa, D. Smith, Studies on adsorption. XI. A system of classification of solution adsorption isotherms and its use in diagnosis of adsorption mechanisms and in measurement of specific surface areas of solids, *J. Chem. Soc. London* 56 (1960) 1973–2993.
- [29] I. Langmuir, The constitution and fundamental properties of solids and liquids, *J. Am. Chem. Soc.* 38 (1916) 2221–2295.
- [30] H.M.F. Freundlich, Over the adsorption in solution, *Z. Phys. Chem.* 57 (1906) 385–471.
- [31] K.V. Kumar, Optimum sorption isotherm by linear and non-linear methods for malachite green onto lemon peel, *Dyes Pigments* 74 (2007) 595–597.
- [32] S. Wang, E. Ariyanto, Competitive adsorption of malachite green and Pb ions on natural zeolite, *J. Colloid Interface Sci.* 314 (2007) 25–31.
- [33] S.S. Tahir, N. Rauf, Removal of a cationic dye from aqueous solutions by adsorption onto bentonite clay, *Chemosphere* 63 (2006) 1842–1848.
- [34] G. Crini, H.N. Peindy, F. Gimbert, C. Robert, Removal of C.I. Basic Green 4 (malachite green) from aqueous solutions by adsorption using cyclodextrin based adsorbent: kinetic and equilibrium studies, *Sep. Purif. Technol.* 53 (2007) 97–110.
- [35] K. Porkodi, K. Vasanth Kumar, Equilibrium, kinetics and mechanism modeling and simulation of basic and acid dyes sorption onto jute fiber carbon: eosin yellow, malachite green and crystal violet single component systems, *J. Hazard. Mater.* 143 (2007) 311–327.
- [36] V.K. Gupta, S.K. Srivastava, D. Mohan, Equilibrium uptake, sorption dynamics, process optimization and column operations for the removal and recovery of malachite green from wastewater using activated carbon and activated slag, *Ind. Eng. Chem. Res.* 36 (1997) 2207–2218.
- [37] A. Mittal, Adsorption kinetics of removal of a toxic dye, malachite green, from wastewater by using hen feathers, *J. Hazard. Mater.* 133 (2006) 196–202.
- [38] I.D. Mall, V.C. Srivastava, N.K. Agarwal, I.M. Mishra, Adsorptive removal of malachite green dye from aqueous solution by bagasse fly ash and activated carbon-kinetic study and equilibrium isotherm analyses, *Colloid Surf. A* 264 (2005) 17–28.
- [39] T.W. Weber, R.K. Chakravorty, Pore and solid diffusion models for fixed-bed adsorbents, *AIChE J.* 20 (1974) 228–238.
- [40] Y. El Mouzdahir, A. Elmchaouri, R. Mahboub, A. Gil, S.A. Korili, Adsorption of methylene blue from aqueous solutions on a moroccan clay, *J. Chem. Eng. Data* 52 (2007) 1621–1625.
- [41] S. Lagergren, About the theory of so-called adsorption of soluble substances, *Kungliga Svenska Vetenskapsakademiens Handlingar* 24 (1898) 1–39.

- [42] Y.S. Ho, G. McKay, Sorption of dye from aqueous solution by peat, *Chem. Eng. J.* 70 (1998) 115–124.
- [43] E. Bulut, M. Ozacar, I.A. Sengil, Adsorption of malachite green onto bentonite: equilibrium and kinetic studies and process design, *Micropor. Mesopor. Mater.* 115 (2008) 234–246.
- [44] G. McKay, Y.S. Ho, The sorption of lead (II) on peat, *Water Res.* 33 (1999) 578–584.
- [45] B.H. Hameed, H. Hakimi, Utilization of durian (*Durio zibethinus* Murray) peel as low cost sorbent for the removal of acid dye from aqueous solutions, *Biochem. Eng. J.* 39 (2008) 338–343.